On the prospects of optical cycling in diatomic cations: Effects of transition metals, spin-orbit couplings, and multiple bonds

Paweł Wójcik,[1] Eric R. Hudson,[2,3] and Anna I. Krylov[1,*]

[1] *Department of Chemistry, University of Southern California, Los Angeles, California 90089, USA*

[2] *Department of Physics and Astronomy, University of California Los Angeles, Los Angeles, California, USA*

[3] *UCLA Center for Quantum Science and Engineering, Los Angeles, California, USA*

(Dated: May 11, 2022)

Molecules with optical cycling centers (OCCs) are highly desirable in the context of fundamental studies as well as applications (e.g., quantum computing) because they can be effectively cooled to very low temperatures by repeated absorption and emission (hence, cycling). Charged species offer additional advantages for experimental control and manipulation. We present a systematic computational study of a series of diatomic radical-cations made of a *d*-block metal and a *p*-block ligand, that are isoelectronic (in their valence shell) to the successfully laser-cooled neutral molecules. Using high-level electronic structure methods, we characterize state and transition properties of low-lying electronic states and compute Franck-Condon factors. The computed branching ratios and radiative lifetimes reveal that the electronic transitions analogous to those successfully used in the laser cooling of neutral molecules are less than optimal in the cations. We propose alternative transitions suitable for optical cycling and highlight trends that could assist future designs of OCCs in charged or neutral molecules.

I. INTRODUCTION

Optical cycling center (OCC) is a chromophore moiety that supports electronic transitions closed for electronic and vibrational decay to other channels. It means that the excited state should decay primarily to the ground electronic state. The transition should also be

* Electronic address: krylov@usc.edu

closed at the vibrational level, such that the excited-state decay populates primarily the ground vibrational state. In this case the system can be subjected to repeated absorption–emission cycles without exciting molecular vibrations. By tuning the photon energy to be slightly below the electronic transition energy, each cycle results in slowing the translational motion of the system. This is the essence of laser cooling. The lower-energy spectral features, such as rotational and fine structure, must also be considered, but it is the closure on the vibronic (vibrational and electronic) level that is the chief prerequisite for optical cycling. The excited electronic state must also be short lived (lifetime <10-100 μs) to afford a rapid photon scattering rate necessary for effective laser cooling (this condition, however, is not critical for working with cations[1]). These requirements for molecules suitable for laser cooling are well known from earlier studies.[1–5] Potential applications of laser-coolable species include quantum computing[6,7] and sensing, as well as precision measurements of fundamental physical constants.[8–11]

Charged particles are particularly attractive for experimental applications because they can be controlled by electric fields, motivating intense experimental and theoretical research in this area. Heavy molecular ions have been investigated as promising platforms for precision measurements.[8–11] In charged molecular species, an OCC is useful for system preparation and measurement.[12] Much experimental and theoretical effort has been focused on the SiO^+ cation.[13–16] Prospective advantages in state control motivate an active search for molecular ions with a large ground-state dipole moment and a splitting of the ground state into opposite parity states in the radio frequency range[17–20]. A closed optical cycle with a radiative lifetime of approximately 110 μs was predicted for the $AcOH^+$ cation.[21] Computational studies have shown that because of high electronic transition energies RaF^+ and RaH^+ cations are not well suited for laser manipulations.[22] Favorable vibrational branching ratios were reported for a transition of TlF^+ lying in the UV region.[23] In the context of precision measurements, highly charged heavy cations offer additional benefits. In this domain the PaF^{3+} cation was identified as a promising candidate for cooling.[24]

The prospects of laser-cooling anions have been discussed. Anions could afford sympathetic cooling of other negatively charged particles.[25] However, in contrast to neutral and cationic species, which support many bound excited states, anions rarely have bound excited states.[26–28] Among promising exceptions[25,29] are C_2^- and BN^-, which are isoelectronic to SiO^+. Molecular anions of alkali metals were also investigated computationally[30,31], how-

ever, the authors were not able to establish whether their electronic states were bound or metastable with respect to electron detachment.

The search for optically cyclable molecular cations is ongoing. Earlier, we investigated diatomic ions of the main group elements with a goal to find transitions suitable for cycling.[1] The results were disappointing—compared to the isoelectronic neutral species with good OCCs, the transitions in the cations generally featured less favorable properties. We attributed this difference to more delocalized electronic structure and higher density of states in the cations, which present challenges in the design of cationic OCCs.[1] Other computational studies have shown that BO^+ and $SiBr^+$ are not promising for laser cooling.[32,33] Here, we extend our search for cyclable molecular cations to a series of diatomic radical-cations comprising a *d*-block metal and a *p*-block ligand that are isoelectronic (in their valence shell) to the successfully laser-cooled neutral molecules.

To assess the suitability of these species for optical cycling, we compute potential energy curves of their low-lying electronic states. We then use these curves to compute respective equilibrium geometries and Franck-Condon factors (FCFs), defined here as the squared overlap between the vibrational states:

$$q_{\nu_I \nu_F} = |\langle \nu_I | \nu_F \rangle|^2, \tag{1}$$

where $|\nu_I\rangle$ and $|\nu_F\rangle$ are the vibrational states of the initial and final electronic states, respectively.

Within the Born-Oppenheimer and Condon approximations, FCFs determine vibrational branching of the electronic transition. The most desired property for optical cycling is a diagonal FCF matrix—so that there is no vibrational branching during electronic decay. Because repumping schemes can mitigate the effect of leaking population, cumulative FCFs—the sum of the first few FCFs with fixed ν_I—are also valuable in evaluating quality of an OCC.[34]

In diatomic molecules, FCFs are determined by the change in the position of the minimum and the curvature of the potential energy curves of the ground and excited states. The position of the minimum (i.e., equilibrium bond length) depends on the bonding pattern, determined by the shape of occupied molecular orbitals. Hence, the change in electron density upon excitation provides a visual cue whether the bonding pattern changes and whether or not one may expect diagonal FCF—i.e., large changes in the inter-atomic charge

distribution are expected to give rise to a significant bond length change and, consequently, non-diagonal FCFs.

The low-lying electronic transitions in doublet electronic states, such as radical-cations studied here, are transitions of the unpaired electron. Hence, we use Dyson orbitals to visualizing the states of the unpaired electron in the ground and excited states[35]:

$$\phi^d(1) = \sqrt{N} \int \Psi^N(1, \ldots, n) \Psi^{N-1}(2, \ldots, n) \, \mathrm{d}2 \ldots \mathrm{d}n \,, \tag{2}$$

where Ψ^N and Ψ^{N-1} are the solution of the electronic Schrödinger equation for a cation (one unpaired electron) and a dication (closed-shell), respectively. The pair of states with Dyson orbitals localized outside of the bond area are likely to have diagonal FCFs. This idea, first introduced by Isaev and Berger[36], has led to successful laser-cooling of polyatomic neutral molecules[37–39]. Following this strategy, more polyatomic molecules were proposed as prospective candidates for laser cooling[40–44].

In this study we follow the same design paradigm as before[1]—seeking molecular cations with a single unpaired electron localized on a metal atom so that electronic transitions resemble atomic transitions on the metal. The atomic-like transitions localized on the metal do not disturb the bonding pattern in a molecule, which should lead to diagonal FCFs[36]. Fig. 1 illustrates the design principle. We first consider cations of third group elements (yttrium or scandium). These metals lose one of their three valence electrons by bonding to a 17^{th} group atom, which requires one electron to reach a closed-shell configuration. To make a cation, the second valence electron is removed leading to a molecule with a positive charge and the desired unpaired electron on the metal. We follow the same strategy to construct other pairs of a metal with n valence electrons and a ligand missing $n - 2$ electrons to a closed-shell, as shown in Fig. 1.

The structure of the paper is the following. The next section describes theoretical methods and computational details. Section III presents the results for the diatomic cations in which we identified atomic-like transitions on the metal atom and reports our best candidate molecules for optical cycling. Our concluding remarks are given in Section IV.

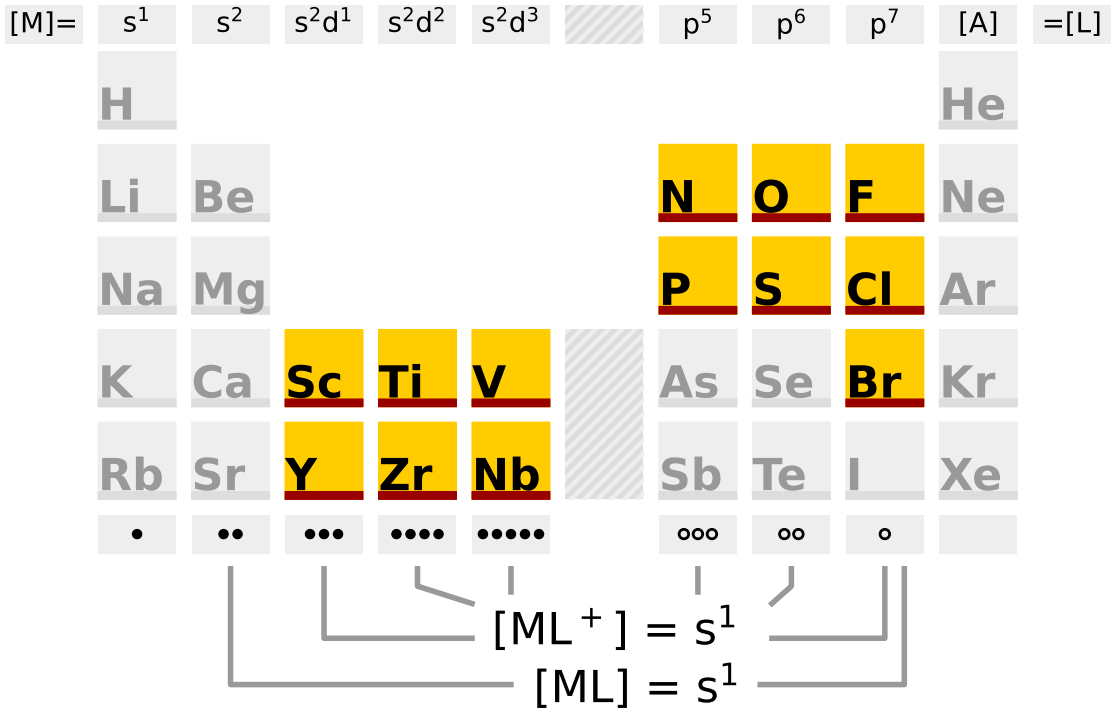

FIG. 1. Electronic design principle of OCCs in diatomic cations investigated in this study. Electronic configurations of radical-cations ML^+ mimic the electronic structure of the successfully laser-cooled neutral molecules ML. In these neutral species, an alkali-earth metal forms an ionic bond with a ligand L (which needs one extra electron to form a closed shell), creating a +1 local charge and a single valence electron localized on the metal. This pattern results in electronic transitions localized on the metal[36]. The top row shows the electronic configurations of the elements in each column. In the bottom row the full and empty dots depict valence electrons and valence holes (electrons needed to complete the shell). Color highlights elements studied in this work.

II. THEORETICAL METHODS AND COMPUTATIONAL DETAILS

We solve the electronic structure problem using high-level *ab initio* methods following the protocols from our previous studies on laser-coolable species.[1,40,41,43] We use the equation-of-motion coupled-cluster method for electron attachment (EOM-EA-CC) to describe the ground and excited electronic states of doublet radical cations[50,51]. In these calculations the target states (with +1 charge) are obtained by attaching an electron to a closed-shell +2 reference state described by the coupled-clusters singles doubles (CCSD) method. This

TABLE I. Basis sets used in this study[a].

atom	basis set
Sc, Ti, V	aug-cc-pwCVTZ[45]
Y, Zr, Nb	aug-cc-pwCVTZ-PP[46]
Y, Zr, Nb	aug-cc-pwCVTZ-DK[46]
F, Cl, Br, O, S, N, P	aug-cc-pVTZ[47–49]

[a] When two basis sets are shown for the same atom, it means that the energy and properties calculations were computed with a basis with an effective core potential and SOCs were computed with an all-electron basis.

approach leads to a balanced description of the ground and excited electronic states and is naturally spin-pure[51]. Table I lists basis sets used in our calculations[52].

Because the ordering of the electronic states is different in different cations (and sometimes changes at different level of theory), we do not use spectroscopic notations (i.e., in which the ground state is labeled by 'X'), but instead simply number each state from 1 in each symmetry irrep (i.e., angular momentum projection group). This convention allows us to use a consistent notation for all molecules.

We include the effect of spin-orbit couplings (SOCs) using the state interaction scheme (sometimes referred to as a perturbative approach): we first compute a set of low-lying non-relativistic EOM-EA-CCSD states and use them to evaluate matrix elements of the Breit-Pauli Hamiltonian (we use mean-field approach to include two-electron contributions)[53,54]. We then construct and diagonalize the matrix of the SOC-perturbed Hamiltonian:

$$(H_0^{EOM} + H^{BP})U = UE^{SOC}, \tag{3}$$

where H_0^{EOM} is a diagonal matrix composed of EOM-EA energies and H^{BP} is the matrix of the Breit-Pauli Hamiltonian in the basis of the EOM-EA states. The resulting energies E^{SOC} are energies of the SOC-perturbed EOM states and matrix U contains the respective eigenstates. This matrix can be used to obtain properties of the SO-perturbed states, such as permanent and transition dipole moments:

$$\mu^{SOC} = U^{\dagger}\mu^{0}U \tag{4}$$

where μ^0 is the matrix of dipole moments calculated in the basis of the non-relativistic EOM-EA-CCSD states. The state-interaction treatment of SOCs becomes exact in the limit where

all electronic states are included in the calculation. In the present study, we considered eight lowest electronic states.

We use the computed spin–orbit corrected potential energy curves to determine equilibrium geometries and to compute FCFs. We do not use harmonic approximations[55] but solve the vibrational problem exactly. Numerical integration of the overlaps between eigenfunctions gives the FCFs.

Einstein's A_{IF} coefficients give the probabilities of a spontaneous decay from an initial state I to a final electronic state F:

$$A_{IF} = \frac{\omega_{IF}^3 \mu_{IF}^2}{3\hbar c^3 \pi \varepsilon_0}, \tag{5}$$

where ω_{IF} is the transition frequency and μ_{IF} is the transition dipole moment. The radiative lifetime of a state I is obtained by summing over all decay channels

$$\tau_I = 1/\sum_F A_{IF}, \tag{6}$$

where the index F goes over all states below state I.

All electronic structure calculations (including energies, state and transition properties) were carried out using *Q-Chem*.[56,57] We computed FCFs with the *LEVEL16* program,[58] which solves the quantum vibrational problem numerically using potential energy curves provided by the user. In these calculations, the interatomic potential is represented by analytic functions: exponential functions (fit to the provided potential energy curves) represent asymptotes and the regions in between the sampled points are interpolated with cubic splines. The complete potential energy curves for both non-relativistic and spin-orbit corrected states are given in the Supplementary Information (SI).

III. RESULTS AND DISCUSSION

A. Y and Sc series

Yttrium and scandium cations feature the sought-after atomic-like spectrum, as clearly illustrated by the Dyson orbitals in Fig. 2. In these representative examples of the YCl^+ and NbN^+ cations, Dyson orbitals strongly resemble atomic D states. The $1^2\Sigma$ and $2^2\Pi$ states correspond to the cation with a singly occupied s- or p-type orbital, respectively,

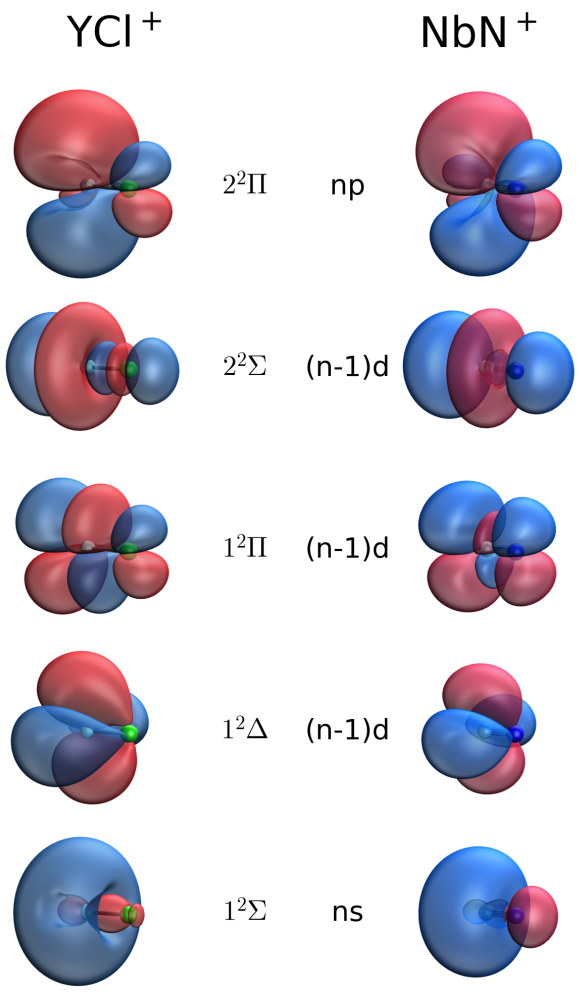

FIG. 2. Dyson orbitals showing the unpaired electron in low-lying electronic states. Representative examples of YCl^+(left) and NbN^+(right) (isovalue = 0.02; plotted with iQmol[59]). In the hydrogen-like orbital labels, the principal quantum number n equals 4 for the Sc, Ti, and V metal cations and 5 for the Y, Zr, and Nb cations.

the $1^2\Delta$, $1^2\Pi$, and $2^2\Sigma$ correspond to a singly occupied d-type orbital. Although atomic states originating from a singly occupied d-type orbital have the same electronic angular momentum, the diatomic states vary with respect to its projection on the molecular axis, giving rise to three types of molecular states. Table II and Fig. 3 show non-relativistic EOM-EA-CCSD excitation energies computed at the ground-state equilibrium geometries for ScF^+, $ScCl^+$, $ScBr^+$, YF^+, YCl^+, and YBr^+.

All states consistently appear in the same order except for the two lowest-lying states. The $1^2\Delta$ is the ground state for scandium cations whereas it lies above the $1^2\Sigma$ state for

TABLE II. Vertical excitation energies (eV) for ScX^+ and YX^+ cations at the ground-state equilibrium geometry. Transition dipole moments μ (a.u.) correspond to the transition involving the ground state. EOM-EA-CCSD without the inclusion of SOC shifts.

	ScF^+		$ScCl^+$		$ScBr^+$		YF^+		YCl^+		YBr^+	
State	E_{ex}	μ	E_{ex}	μ	E_{ex}	μ	E_{ex}	μ	E_{ex}	μ	E_{ex}	μ
$1^2\Delta$	**0.000**	—	**0.000**	—	**0.000**	—	0.634	0.000	0.620	0.000	0.536	0.000
$1^2\Sigma$	0.502	0.000	0.143	0.000	0.032	0.000	**0.000**	—	**0.000**	—	**0.000**	—
$1^2\Pi$	0.781	0.141	0.431	0.138	0.348	0.144	1.427	0.923	1.129	0.745	1.056	0.593
$2^2\Sigma$	2.058	0.000	1.615	0.000	1.471	0.000	2.160	1.213	1.658	1.125	1.684	0.912
$2^2\Pi$	4.897	0.578	4.458	0.555	4.216	0.551	3.829	1.951	3.612	1.906	3.759	1.692
r_e (Å)	1.79		2.21		2.34		1.90		2.35		2.46	

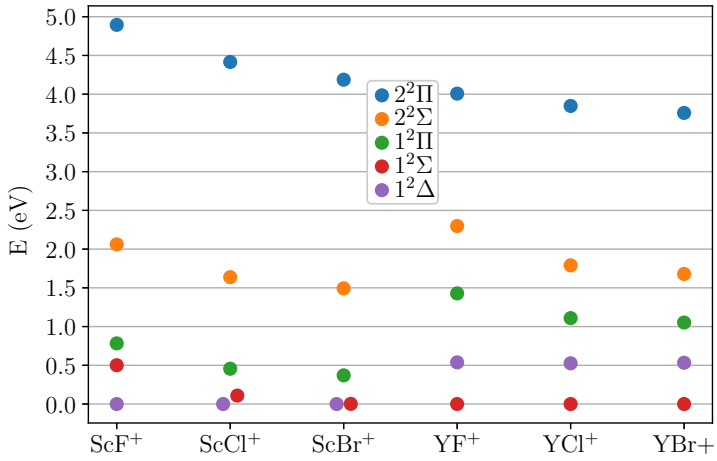

FIG. 3. Scandium and yttrium halide cations with low-lying localized doublet states. Vertical excitation energies (EOM-EA-CCSD energies without the inclusion of SOC shifts) at the ground-state minimum.

yttrium cations. By inspecting Table II and Fig. 3, we observe a general trend—that the energy gaps increase with the increasing electron-withdrawing strength of the halogen ligand. This ability to tune up OCC properties by tuning the ligand's electron-withdrawing strength was discussed in previous computational studies[40,44].

We first assess whether the $2^2\Pi \rightarrow 1^2\Sigma$ transition (analog of the atomic $^2P \rightarrow {}^2S$ transition) is suitable for optical cycling. Just as in the case of neutral molecules, this transition

is characterized by a highly diagonal FCFs (see Table S3 in the SI). The large excitation energy ($\approx$ 4 eV) and a strong transition dipole moment give rise to a short radiative lifetime of the excited state. Unfortunately, these advantageous properties come together with undesired ones. First, there are intermediate states, which can drain the populations out of the OCC. Second, the excitation energy of this transition is in an undesirable UV range. This transition is even less attractive in the case of the scandium cations, where the $1^2\Sigma$ state is an excited state. Our calculations indicate that the YF^+ cation, the best candidate in this group shown in Fig. 4, is unlikely to form a good OCC.

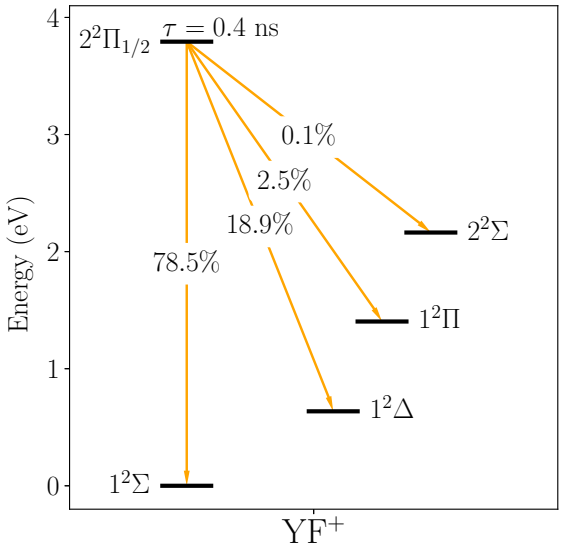

FIG. 4. YF^+ is the most diagonal cation for the $2^2\Pi \rightarrow 1^2\Sigma$ transition. Numbers on the arrows indicate branching ratios. The four decay channels generate population leakage out of the cycling transition which is undesired in an OCC.

The simplest way to avoid electronic branching decays is to use the transition between the ground and the first excited electronic states. Unfortunately the transition between $1^2\Sigma$ and $1^2\Delta$ states is dipole forbidden. However, the SOCs can mix non-relativistic states, giving rise to a non-vanishing transition dipole moment, which might be sufficiently large to allow for optical cycling.

Tables S2 and S1 shows the SOC-corrected states with their energies, transition dipole moments, and radiative lifetimes. SOCs mix the non-relativistic states and the extent of mixing is determined by the energy gaps between the states (which varies between the

cations) and the magnitude of the Breit-Pauli Hamiltonian matrix elements (which are larger for cations containing heavier atoms). The energy shifts due to the SOCs do not exceed 0.1 eV and cause splittings of the Π and Δ states. Crucially, the SOC-perturbed states show non-vanishing transition dipole moments between the Δ and Σ states in the range of 0.01 a.u.

Consequently, we consider the $1^2\Delta_{3/2} \rightarrow 1^2\Sigma_{1/2}$ transition as the second candidate for an OCC. This transition is characterized by the excitation energy of about 0.75 eV and a transition dipole moment of 0.03 a.u., yielding the radiative lifetimes longer than hundreds μs. The FCFs saturate slowly, with the most diagonal YCl^+ cation reaching 0.9989 at four states, as shown in Tables S4 and S5 in the SI. Because of the long radiative lifetime and large vibrational branching, using this transition for optical cycling is challenging. However, the fact that the inclusion of SOCs can open a way for cycling on a formally forbidden transition motivates the inspection of similar transitions in other cations.

B. Other groups: Ti or Zr with chalcogens, and V or Nb with N or P

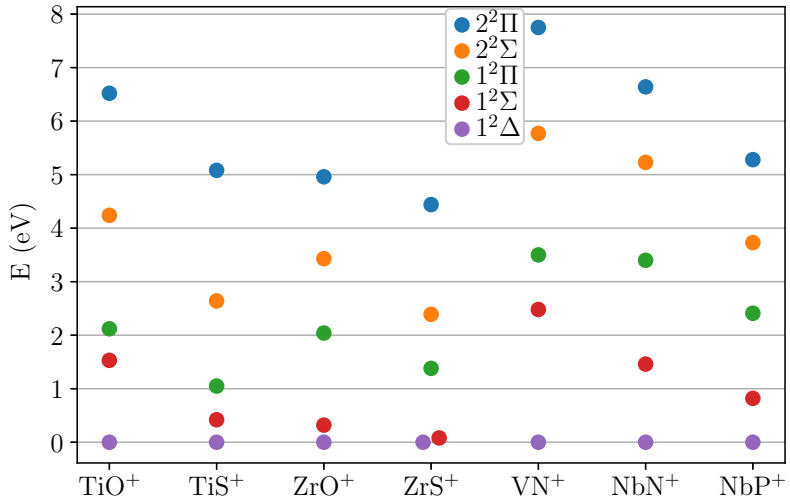

FIG. 5. Multiply bonded cations with low-lying localized doublet states. Vertical excitation energies (EOM-EA-CCSD energies without the inclusion of SOC shifts) at the ground-state equilibrium geometry.

The spectra of the multiply bonded cations are similar to those of the scandium cations

discussed above. All species feature the $1^2\Delta$ ground state followed by the $1^2\Sigma$ and $1^2\Pi$ states. Again, we observe an increase in the energy gaps with an increasing electron withdrawing strength of the ligand. Additionally, a new trend becomes apparent—the excitation energies increase with the number of bonds in the cation, as shown in Fig. 5. In the case of the transition from yttrium to zirconium and niobium cations, where the order of the ground and the first excited states changes, taking the energy of $1^2\Delta$ state as the reference point allows to observe a consistent increase. This new trend is particularly apparent for the series F, O, and N as the ligands or Cl, S, and P, shown in Figs. S1 and S2 in the SI.

In this set of cations we again inspect the transition between the ground and the first excited states. The increased energy gaps in Ti and V relative to Sc improve the radiative lifetimes. The heavy atoms Zr and Nb also have stronger SOCs, which increases transition dipole moment, but an improvement in the radiative lifetime is achieved only for Nb as in the Zr cations the $1^2\Delta$ and $1^2\Sigma$ states become nearly degenerate. The small improvement in the radiative lifetime of the $1^2\Sigma \rightarrow 1^2\Delta_{3/2}$ transition in multiply bonded cations is accompanied by a large improvement in the diagonality of the corresponding FCFs, Sec. S3 in the SI, making this transition very a promising OCC. The best candidate in this group is the NbN^+ cation, with FCFs summarized in Table III and the radiative lifetime τ= 77 μs.

In search for a shorter radiative lifetime, we focus on the dipole-allowed transition. As the last candidate for an OCC we consider a three-level cycle with the $1^2\Pi$ excited state decaying to the ground $1^2\Delta$ and an intermediate $1^2\Sigma$ states. The FCFs on the $1^2\Pi_{1/2} \rightarrow 1^2\Delta_{3/2}$ transition single out zirconium and scandium cations where the sum of the first four FCFs reaches 0.9999; the titanium cations also reach such saturation by adding the fifth FCF (see Section S4 in the SI). In all these cations, the excited state decays $\approx 60\%$ to the intermediate $1^2\Sigma$ state. To take advantage of the rapid cycling offered by the short lifetime of the excited state, this intermediate state must be repumped. Diagonal FCFs, necessary for an efficient repumping, render the ZrO^+ cation to be the most appealing candidate for the three-level OCC.

We do not report details about other screened cations because our calculations suggest that they do not feature the localized transitions. Cations of Cr or Mo with a C or Si have very different electronic structure, with significant multi-configurational character; their corresponding dications do not converge to a singlet state. We detected similar problems for Ti or Zr with Se cations as well as V and Nb with As cations.

C. FCFs, electronic charge displacement, and Dyson orbitals

The transition between the $2^2\Pi$ and $1^2\Sigma$ states is known for its diagonal FCFs, which are attributed to the localized character of the transition. The localized transition preserves the charge distribution in the interatomic area of both states leading to similar bond lengths. We interpret the bond length changes of other electronic transitions using similar analysis applied to the changes in shapes of the Dyson orbitals.

The $1^2\Sigma \rightarrow 1^2\Delta$ transition is most promising as it involves the ground and the first excited electronic states avoiding branching to intermediate levels. The electronic density changes from a spherical distribution of the *s*-orbital to a clover-shaped shape of the *d* orbital, see Fig. 2. For most of the yttrium and scandium cations this transition features FCFs indicative of the expected significant vibrational branching (see Tables S5 and S4 in the SI). For all multiply bonded cations except for ZrS^+ this is one of the most diagonal transitions that we found (Tables S6–S9 in the SI).

In the dipole-allowed $1^2\Pi \rightarrow 1^2\Delta$ transition, the *d*-orbital on a metal atom changes its alignment from the one that is along the bond to the perpendicular one (Fig. 2). This charge displacement leads to the expected poor FCFs, with a few exceptions of scandium or zirconium cations where the sum the first four FCFs differs from unity by less than 10^{-4} (see Sec. S4 in the SI).

This analysis suggests that a disruption in the electronic density of the bond area does not nessessarily render the transition to be unusable for optical cycling. One possible reason is that the presence of a multiple bond is a structurally stabilizing factor.

D. Best candidates for optical cycling

The variations of the spectra introduced by states derived from a singly occupied *d*-type orbital led us to consider four types of OCCs. The molecular analog of the atomic $^2P \rightarrow {}^2S$ transition was deemed not promising (see Section III A in the SI). Among the low-lying states we considered the transitions between the first excited and the ground states, separately for ground $1^2\Sigma$ and for ground $1^2\Delta$ cations, as well as a three level scheme involving the second excited $1^2\Pi$ state. We present the best candidates in each of these groups in Fig. 6; Table III summarizes the corresponding FCFs.

TABLE III. FCFs for the best candidates[a].

YCl^+ $1^2\Delta_{3/2} \rightarrow 1^2\Sigma_{1/2}$			ZrO^+ $1^2\Pi_{1/2} \rightarrow 1^2\Delta_{3/2}$			NbN^+ $1^2\Sigma_{1/2} \rightarrow 1^2\Delta_{3/2}$		
	$q_{\nu_i\nu_f}$	sum		$q_{\nu_i\nu_f}$	sum		$q_{\nu_i\nu_f}$	sum
q_{00}	0.916	0.9165	q_{00}	0.744	0.7444	q_{00}	0.985	0.9851
q_{01}	0.082	0.9985	q_{01}	0.224	0.9687	q_{01}	0.015	1.0000
q_{02}	0.000	0.9987	q_{02}	0.029	0.9978	q_{02}	0.000	1.0000
q_{03}	0.000	0.9989	q_{03}	0.002	0.9999	q_{03}	0.000	1.0000

Numerical solution of the quantum vibrational problem using spin-orbit perturbed EOM-EA-CCSD potential energy surfaces.

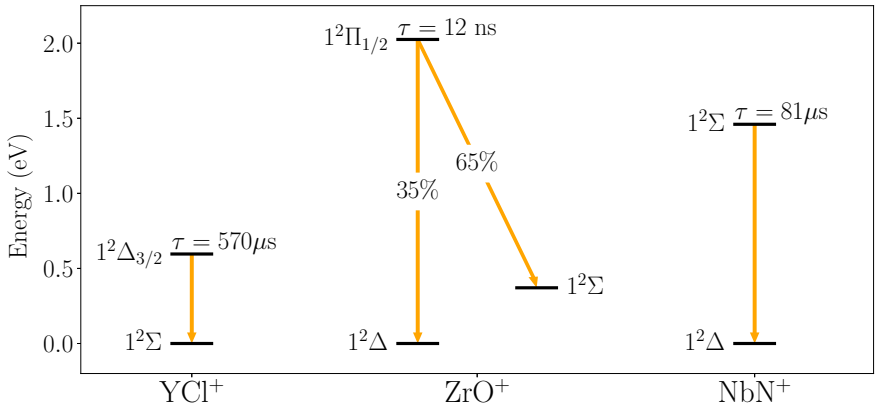

FIG. 6. The best candidates in each of the three types of a laser cooling scheme. In the group of the cations with the $1^2\Sigma$ ground state, the YCl^+ molecule shows the most diagonal transition. In the group of the cations with the $1^2\Delta$ ground state and highly diagonal transitions, the NbN^+ cation stands out with the shortest radiative lifetime. The FCFs for the formally dipole-allowed transition between the ground and the second excited state favor scandium and zirconium cations. Large decay to the intermediate state requires also the side branch $1^2\Pi_{1/2} \rightarrow 1^2\Sigma$ transition to show quickly saturating FCFs. This second requirement renders the ZrO^+ cation as the best candidate in this group.

IV. CONCLUSIONS

By using high-level *ab initio* calculations, we investigated series of diatomic radical cations designed to create a localized electronic transition suitable for optical cycling. The results

demonstrate that the localized electronic excitation picture exploited in OCCs in neutral molecules[38,40,41,60–75] to some extent holds for isoelectronic cations formed by transition-metal atoms. This result applies to molecular cations that either contain a transition metal atom or have multiple bonds, which is different from the behavior of other cations[1].

The observed trends can help in designing transitions with desired excitation energy. In multiply bonded cations, we observe persistent diagonal FCFs that are promising for optical cycling, on the $1^2\Sigma_{1/2} \rightarrow 1^2\Delta_{3/2}$ transition. Finally, our analysis of FCFs of selected transitions together with an inspection of the Dyson orbitals of involved states suggests that although the charge displacement often makes the transition unlikely for optical cycling, it is not the crucial design factor. The most promising schemes (summarized in Sec. III D) are: $1^2\Delta_{3/2} \rightarrow 1^2\Sigma$ in YCl^+, $1^2\Pi_{1/2} \rightarrow 1^2\Delta$ with a side branch $1^2\Pi_{1/2} \rightarrow 1^2\Sigma$ in ZrO^+ and $1^2\Sigma \rightarrow 1^2\Delta$ in NbN^+.

Our results can assist engineering of OCCs in other neutral or charged molecules. In particular, a shortening of the radiative lifetime in the most promising $1^2\Sigma \rightarrow 1^2\Delta$ scheme appears possible. The radiative lifetime of an excited state becomes shorter with an increase in either the excitation energy or the transition dipole moment. A use of polyatomic ligands of an electron withdrawing strength exceeding that of atoms appears as the most practical way of raising transition energy. The excitation energy can be further increased with the growing number of the metal-ligand bonds. Similarly, a formally dipole forbidden transition can become sufficiently bright in molecules with heavy nuclei due to an increased SOCs. We expect that the heavy metal analogs of the systems studies in this work (Lu, Hf, Ta cations) are likely to feature fast OCCs on a transition between its low-lying doublet states and that the design principle outlined before should help in its fine-tuning.

ACKNOWLEDGMENTS

This study was funded through the "Molecules Functionalized with Optical Cycling Centers" collaboration, supported by the U.S. Department of Energy (Award DE-SC0019245).

The authors declare the following competing financial interest(s): A.I.K. is the president and a part-owner of Q-Chem, Inc.

[1] M. V. Ivanov, T.-C. Jagau, G.-Z. Zhu, E. R. Hudson, and A. I. Krylov, In search of molecular ions for optical cycling: A difficult road, Phys. Chem. Chem. Phys. **22**, 17075 (2020).

[2] M. D. Di Rosa, Laser-cooling molecules, Eur. Phys. J. D **31**, 395 (2004).

[3] D. McCarron, Laser cooling and trapping molecules, J. Phys. B **51**, 212001 (2018).

[4] N. Fitch and M. Tarbutt, Laser-cooled molecules, Adv. At. Mol. Opt. Phys. **70**, 157 (2021).

[5] P. Yu, A. Lopez, W. A. Goddard III, and N. R. Hutzler, Multi-electron optical cycling centers in polyatomic molecules, preprint (2022).

[6] V. V. Albert, J. P. Covey, and J. Preskill, Robust encoding of a qubit in a molecule, Phys. Rev. X **10**, 031050 (2020).

[7] A. I. Krylov, J. Doyle, and K.-K. Ni, A preface for a themed PCCP collection on quantum information science, Phys. Chem. Chem. Phys. **23**, 6341 (2021).

[8] W. B. Cairncross, D. N. Gresh, M. Grau, K. C. Cossel, T. S. Roussy, Y. Ni, Y. Zhou, J. Ye, and E. A. Cornell, Precision Measurement of the Electron's Electric Dipole Moment Using Trapped Molecular Ions, Phys. Rev. Lett. **119**, 153001 (2017).

[9] N. R. Hutzler, Polyatomic molecules as quantum sensors for fundamental physics, Quantum Sci. Technol. **5**, 044011 (2020).

[10] D. Maison, L. Skripnikov, V. Flambaum, and M. Grau, Search for CP-violating nuclear magnetic quadrupole moment using the $LuOH^+$ cation, J. Chem. Phys. **153**, 224302 (2020).

[11] L. V. Skripnikov, N. S. Mosyagin, A. V. Titov, and V. V. Flambaum, Actinide and lanthanide molecules to search for strong CP-violation, Phys. Chem. Chem. Phys. **22**, 18374 (2020).

[12] C.-Y. Lien, C. M. Seck, Y.-W. Lin, J. H. V. Nguyen, D. A. Tabor, and B. C. Odom, Broadband optical cooling of molecular rotors from room temperature to the ground state, Nat. Comm. **5**, 1 (2014).

[13] P. R. Stollenwerk, I. O. Antonov, S. Venkataramanababu, Y. Lin, and B. C. Odom, Cooling of a zero-nuclear-spin molecular ion to a selected rotational state, Phys. Rev. Lett. **125**, 113201 (2020).

[14] G. Z. Zhu, G. Lao, C. Ho, W. C. Campbell, and E. R. Hudson, High-resolution laser-induced fluorescence spectroscopy of $^{28}Si^{16}O^+$ and $^{28}Si^{16}O^+$ in a cryogenic buffer-gas cell, J. Molec. Spect. , 111582 (2022).

[15] Z. Qin, T. Bai, J. Zhao, and L. Liu, Transition properties between low-lying electronic states of SiO^+, J. Molec. Spect. **370**, 111298 (2020).

[16] R. Li, X. Yuan, G. Liang, Y. Wu, J. Wang, and B. Yan, Laser cooling of the SiO^+ molecular ion: A theoretical contribution, Chem. Phys. **525**, 110412 (2019).

[17] M. Mills, H. Wu, E. C. Reed, L. Qi, K. R. Brown, C. Schneider, M. C. Heaven, W. C. Campbell, and E. R. Hudson, Dipole–phonon quantum logic with alkaline-earth monoxide and monosulfide cations, Phys. Chem. Chem. Phys. **22**, 24964 (2020).

[18] E. R. Hudson and W. C. Campbell, Dipolar quantum logic for freely rotating trapped molecular ions, Phys. Rev. A **98**, 040302 (2018).

[19] W. C. Campbell and E. R. Hudson, Dipole-phonon quantum logic with trapped polar molecular ions, Phys. Rev. Lett. **125**, 120501 (2020).

[20] E. R. Hudson and W. C. Campbell, Laserless quantum gates for electric dipoles in thermal motion, Phys. Rev. A **104**, 042605 (2021).

[21] A. V. Oleynichenko, L. V. Skripnikov, A. V. Zaitsevskii, and V. V. Flambaum, Laser-coolable $AcOH^+$ ion for $\mathcal{CP}$-violation searches, Phys. Rev. A **105**, 022825 (2022).

[22] T. A. Isaev, S. G. Wilkins, and M. Athanasakis-Kaklamanakis, On the Feasibility of Rovibrational Laser Cooling of Radioactive RaF^+ and RaH^+ Cations, Atoms **9**, 101 (2021).

[23] W. Chmaisani and S. Elmoussaoui, Theoretical study of laser cooling of the TlF^+ molecular ion, Phys. Chem. Chem. Phys. **23**, 1718 (2021).

[24] C. Zülch, K. Gaul, S. M. Giesen, R. F. G. Ruiz, and R. Berger, Cool molecular highly charged ions for precision tests of fundamental physics, arXiv preprint arXiv:2203.10333 (2022).

[25] P. Yzombard, M. Hamamda, S. Gerber, M. Doser, and D. Comparat, Laser cooling of molecular anions, Phys. Rev. Lett. **114**, 213001 (2015).

[26] G. L. Gutsev, M. Nooijen, and R. J. Bartlett, Valence and excited dipole-bound states of polar diatomic anions: LiH^-, LiF^-, $LiCl^-$, NaH^-, NaF^-, $NaCl^-$, BeO^-, and MgO^-, Chem. Phys. Lett. **276**, 13 (1997).

[27] W. Skomorowski, S. Gulania, and A. I. Krylov, Bound and continuum-embedded states of cyanopolyyne anions, Phys. Chem. Chem. Phys. **20**, 4805 (2018).

[28] Y. Lu, R. Tang, and C. Ning, Observation of an Excited Dipole-Bound State in a Diatomic Anion, J. Phys. Chem. Lett. **12**, 5897 (2021).

[29] S. Liu, G. Wang, Y. Li, X. Li, W. Huang, and E. Feng, Theoretical investigation of laser

cooling for BN^- anion by ab inito calculation, Spectrochim. Acta Part A **255**, 119670 (2021).

[30] I. Zeid, N. El-Kork, Sally Al Shawa, and M. Korek, Theoretical study of the alkali hydride anions XH^- (X= Li, Na, and K), Chem. Phys. **538**, 110825 (2020).

[31] A. Moussa, N. El-Kork, and M. Korek, Laser cooling and electronic structure studies of CaK and its ions $CaK^{\pm}$, New J. Phys. **23**, 013017 (2021).

[32] Y. Liu, L. Xiao, Y. Liu, and B. Yan, Theoretical study of laser cooling of the BO^+ molecular ion, J. Quant. Spectrosc. Radiat. Transf. **280**, 108102 (2022).

[33] L. Li, Y. Liu, and B. Yan, Spectroscopy and laser cooling of $SiBr^+$: A computational perspective, Spectrochim. Acta Part A **273**, 121042 (2022).

[34] C. Zhang, H. Korslund, Y. Wu, S. Ding, and L. Cheng, Towards accurate prediction for laser-coolable molecules: relativistic coupled-cluster calculations for yttrium monoxide and prospects for improving its laser cooling efficiencies, Phys. Chem. Chem. Phys. **22**, 26167 (2020).

[35] A. I. Krylov, From orbitals to observables and back, J. Chem. Phys. **153**, 080901 (2020).

[36] T. A. Isaev and R. Berger, Polyatomic candidates for cooling of molecules with lasers from simple theoretical concepts, Phys. Rev. Lett. **116**, 063006 (2016).

[37] I. Kozyryev, L. Baum, K. Matsuda, and J. M. Doyle, Proposal for laser cooling of complex polyatomic molecules, ChemPhysChem **17**, 3641 (2016).

[38] I. Kozyryev, L. Baum, K. Matsuda, B. L. Augenbraun, L. Anderegg, A. P. Sedlack, and J. M. Doyle, Sisyphus laser cooling of a polyatomic molecule, Phys. Rev. Lett. **118**, 173201 (2017).

[39] D. Mitra, N. B. Vilas, C. Hallas, L. Anderegg, B. L. Augenbraun, L. Baum, C. Miller, S. Raval, and J. M. Doyle, Direct laser cooling of a symmetric top molecule, **369**, 1366 (2020).

[40] M. V. Ivanov, F. H. Bangerter, and A. I. Krylov, Towards a rational design of laser-coolable molecules: Insights from equation-of-motion coupled-cluster calculations, Phys. Chem. Chem. Phys. **21**, 19447 (2019).

[41] M. V. Ivanov, S. Gulania, and A. I. Krylov, Two cycling centers in one molecule: Communication by through-bond interactions and entanglement of the unpaired electrons, J. Phys. Chem. Lett. **11**, 1297 (2020).

[42] M. Ivanov, A. I. Krylov, and S. Zilberg, Long-range N-N bonding by Rydberg electrons, J. Phys. Chem. Lett. **11**, 2284 (2020).

[43] M. V. Ivanov, F. H. Bangerter, P. Wójcik, and A.I. Krylov, Towards ultracold organic chem-

istry: Prospects of laser cooling large organic molecules, J. Phys. Chem. Lett. **11**, 6670 (2020).

[44] G. Z. Zhu, D. Mitra, B. L. Augenbraun, C. E. Dickerson, M. J. Frim, G. Lao, Z. D. Lasner, A. N. Alexandrova, W. C. Campbell, J. R. Caram, J. M. Doyle, and E. R. Hudson, Functionalizing aromatic compounds with optical cycling centers, arXiv preprint arXiv:2202.01881 (2022).

[45] N. B. Balabanov and K. A. Peterson, Basis set limit electronic excitation energies, ionization potentials, and electron affinities for the 3*d* transition metal atoms: Coupled cluster and multireference methods, J. Chem. Phys. **125**, 074110 (2006).

[46] K. A. Peterson, D. Figgen, M. Dolg, and H. Stoll, Energy-consistent relativistic pseudopotentials and correlation consistent basis sets for the 4d elements y–pd, J. Chem. Phys. **126**, 124101 (2007).

[47] T. H. Dunning, Jr., Gaussian basis sets for use in correlated molecular calculations. I. The atoms boron through neon and hydrogen, J. Chem. Phys. **90**, 1007 (1989).

[48] R. A. Kendall, T. H. Dunning, Jr., and R. J. Harrison, Electron affinities of the first-row atoms revisited. Systematic basis sets and wavefunctions, J. Chem. Phys. **96**, 6796 (1992).

[49] A. K. Wilson, D. E. Woon, K. A. Peterson, and T. H. Dunning, Gaussian basis sets for use in correlated molecular calculations. ix. the atoms gallium through krypton, J. Chem. Phys. **110**, 7667 (1999).

[50] A. I. Krylov, Equation-of-motion coupled-cluster methods for open-shell and electronically excited species: The hitchhiker's guide to Fock space, Annu. Rev. Phys. Chem. **59**, 433 (2008).

[51] A. I. Krylov, The quantum chemistry of open-shell species, in *Reviews in Comp. Chem.*, edited by A. L. Parrill and K. B. Lipkowitz, volume 30, pages 151–224. J. Wiley & Sons, 2017.

[52] B. P. Pritchard, D. Altarawy, B. Didier, T. D. Gibson, and T. L. Windus, New basis set exchange: An open, up-to-date resource for the molecular sciences community, J. Chem. Inf. Model. **59**, 4814 (2019).

[53] E. Epifanovsky, K. Klein, S. Stopkowicz, J. Gauss, and A. I. Krylov, Spin-orbit couplings within the equation-of-motion coupled-cluster framework: Theory, implementation, and benchmark calculations, J. Chem. Phys. **143**, 064102 (2015).

[54] P. Pokhilko, E. Epifanovsky, and A. I. Krylov, General framework for calculating spin–orbit couplings using spinless one-particle density matrices: theory and application to the equation-

of-motion coupled-cluster wave functions, J. Chem. Phys. **151**, 034106 (2019).

[55] S. Gozem and A. I. Krylov, The ezSpectra suite: An easy-to-use toolkit for spectroscopy modeling, WIREs: Comput. Mol. Sci. **12**, e1546 (2022).

[56] A. I. Krylov and P. M. W. Gill, Q-Chem: An engine for innovation, WIREs: Comput. Mol. Sci. **3**, 317 (2013).

[57] E. Epifanovsky, T. B. Gilbert, X. Feng, J. Lee, Y. Mao, N. Mardirossian, P. Pokhilko, A. F. White, M. P. Coons, A. L. Dempwolff, Z. Gan, D. Hait, P. R. Horn, L. D. Jacobson, I. Kaliman, J. Kussmann, A. W. Lange, K. U. Lao, D. S. Levine, J. Liu, S. C. McKenzie, A. F. Morrison, K. D. Nanda, F. Plasser, D. R. Rehn, M. L. Vidal, Z.-Q. You, Y. Zhu, B. Alam, B. J. Albrecht, A. Aldossary, E. Alguire, J. H. Andersen, V. Athavale, D. Barton, K. Begam, A. Behn, N. Bellonzi, Y. A. Bernard, E. J. Berquist, H. G. A. Burton, A. Carreras, K. Carter-Fenk, R. Chakraborty, A. D. Chien, K. D. Closser, V. Cofer-Shabica, S. Dasgupta, M. de Wergifosse, J. Deng, M. Diedenhofen, H. Do, S. Ehlert, P.-T. Fang, S. Fatehi, Q. Feng, T. Friedhoff, J. Gayvert, Q. Ge, G. Gidofalvi, M. Goldey, J. Gomes, C. E. González-Espinoza, S. Gulania, A. O. Gunina, M. W. D. Hanson-Heine, P. H. P. Harbach, A. Hauser, M. F. Herbst, M. Hernández Vera, M. Hodecker, Z. C. Holden, S. Houck, X. Huang, K. Hui, B. C. Huynh, M. Ivanov, A. Jász, H. Ji, H. Jiang, B. Kaduk, S. Kähler, K. Khistyaev, J. Kim, G. Kis, P. Klunzinger, Z. Koczor-Benda, J. H. Koh, D. Kosenkov, L. Koulias, T. Kowalczyk, C. M. Krauter, K. Kue, A. Kunitsa, T. Kus, I. Ladjánszki, A. Landau, K. V. Lawler, D. Lefrancois, S. Lehtola, R. R. Li, Y.-P. Li, J. Liang, M. Liebenthal, H.-H. Lin, Y.-S. Lin, F. Liu, K.-Y. Liu, M. Loipersberger, A. Luenser, A. Manjanath, P. Manohar, E. Mansoor, S. F. Manzer, S.-P. Mao, A. V. Marenich, T. Markovich, S. Mason, S. A. Maurer, P. F. McLaughlin, M. F. S. J. Menger, J.-M. Mewes, S. A. Mewes, P. Morgante, J. W. Mullinax, K. J. Oosterbaan, G. Paran, A. C. Paul, S. K. Paul, F. Pavošević, Z. Pei, S. Prager, E. I. Proynov, A. Rák, E. Ramos-Cordoba, B. Rana, A. E. Rask, A. Rettig, R. M. Richard, F. Rob, E. Rossomme, T. Scheele, M. Scheurer, M. Schneider, N. Sergueev, S. M. Sharada, W. Skomorowski, D. W. Small, C. J. Stein, Y.-C. Su, E. J. Sundstrom, Z. Tao, J. Thirman, G. J. Tornai, T. Tsuchimochi, N. M. Tubman, S. P. Veccham, O. Vydrov, J. Wenzel, J. Witte, A. Yamada, K. Yao, S. Yeganeh, S. R. Yost, A. Zech, I. Y. Zhang, X. Zhang, Y. Zhang, D. Zuev, A. Aspuru-Guzik, A. T. Bell, N. A. Besley, K. B. Bravaya, B. R. Brooks, D. Casanova, J.-D. Chai, S. Coriani, C. J. Cramer, G. Cserey, A. E. DePrince, R. A. DiStasio, A. Dreuw, B. D. Dunietz, T. R. Furlani,

W. A. Goddard, S. Hammes-Schiffer, T. Head-Gordon, W. J. Hehre, C.-P. Hsu, T.-C. Jagau, Y. Jung, A. Klamt, J. Kong, D. S. Lambrecht, W. Liang, N. J. Mayhall, C. W. McCurdy, J. B. Neaton, C. Ochsenfeld, J. A. Parkhill, R. Peverati, V. A. Rassolov, Y. Shao, L. V. Slipchenko, T. Stauch, R. P. Steele, J. E. Subotnik, A. J. W. Thom, A. Tkatchenko, D. G. Truhlar, T. Van Voorhis, T. A. Wesolowski, K. B. Whaley, H. L. Woodcock, P. M. Zimmerman, S. Faraji, P. M. W. Gill, M. Head-Gordon, J. M. Herbert, and A. I. Krylov, Software for the frontiers of quantum chemistry: An overview of developments in the Q-Chem 5 package, J. Chem. Phys. **155**, 084801 (2021).

[58] R. J. Le Roy, LEVEL: A computer program for solving the radial schrödinger equation for bound and quasibound levels, J. Quant. Spectrosc. Radiat. Transf. **186**, 167 (2017).

[59] A. T. B. Gilbert, IQmol molecular viewer, http://iqmol.org.

[60] E. S. Shuman, J. F. Barry, and D. DeMille, Laser cooling of a diatomic molecule, Nature **467**, 820 (2010).

[61] J. F. Barry, D. J. McCarron, E. B. Norrgard, M. H. Steinecker, and D. DeMille, Magneto-optical trapping of a diatomic molecule, Nature **512**, 286 (2014).

[62] M. T. Hummon, M. Yeo, B. K. Stuhl, A. L. Collopy, Y. Xia, and J. Ye, 2D magneto-optical trapping of diatomic molecules, Phys. Rev. Lett. **110**, 143001 (2013).

[63] A. L. Collopy, S. Ding, Y. Wu, I. A. Finneran, L. Anderegg, B. L. Augenbraun, J. M. Doyle, and J. Ye, 3D magneto-optical trap of yttrium monoxide, Phys. Rev. Lett. **121**, 213201 (2018).

[64] S. Ding, Y. Wu, I. A. Finneran, J. J. Burau, and J. Ye, Sub-Doppler cooling and compressed trapping of YO molecules at μ K temperatures, Phys. Rev. X **10**, 021049 (2020).

[65] V. Zhelyazkova, A. Cournol, T. E. Wall, A. Matsushima, J. J. Hudson, E. A. Hinds, M. R. Tarbutt, and B. E. Sauer, Laser cooling and slowing of CaF molecules, Phys. Rev. A **89**, 053416 (2014).

[66] S. Truppe, H. J. Williams, M. Hambach, L. Caldwell, N. J. Fitch, E. A. Hinds, B. E. Sauer, and M. R. Tarbutt, Molecules cooled below the Doppler limit, Nat. Phys. **13**, 1173 (2017).

[67] J. Lim, J. R. Almond, M. A. Trigatzis, J. A. Devlin, N. J. Fitch, B. E. Sauer, M. R. Tarbutt, and E. A. Hinds, Laser cooled YbF molecules for measuring the electron's electric dipole moment, Phys. Rev. Lett. **120**, 123201 (2018).

[68] X. Alauze, J. Lim, M. A. Trigatzis, S. Swarbrick, F. J. Collings, N. J. Fitch, B. E. Sauer, and

M. R. Tarbutt, An ultracold molecular beam for testing fundamental physics, Quantum Sci. Technol. **6**, 044005 (2021).

[69] B. L. Augenbraun, Z. D. Lasner, A. Frenett, H. Sawaoka, C. Miller, T. C. Steimle, and J. M. Doyle, Laser-cooled polyatomic molecules for improved electron electric dipole moment searches, New J. Phys. **22**, 022003 (2020).

[70] L. Baum, N. B. Vilas, C. Hallas, B. L. Augenbraun, S. Raval, D. Mitra, and J. M. Doyle, 1D magneto-optical trap of polyatomic molecules, Phys. Rev. Lett. **124**, 133201 (2020).

[71] N. B. Vilas, C. Hallas, L. Anderegg, P. Robichaud, A. Winnicki, D. Mitra, and J. M. Doyle, Magneto-Optical Trapping and Sub-Doppler Cooling of a Polyatomic Molecule, arXiv preprint arXiv:2112.08349 (2021).

[72] R. L. McNally, I. Kozyryev, S. Vazquez-Carson, K. Wenz, T. Wang, and T. Zelevinsky, Optical cycling, radiative deflection and laser cooling of barium monohydride (BaH), New J. Phys. (2020), DOI: 10.1088/1367-2630/aba3e9.

[73] T. Chen, W. Bu, and B. Yan, Radiative deflection of a BaF molecular beam via optical cycling, Phys. Rev. A **96**, 053401 (2017).

[74] R. Albrecht, M. Scharwaechter, T. Sixt, L. Hofer, and T. Langen, Buffer-gas cooling, high-resolution spectroscopy, and optical cycling of barium monofluoride molecules, Phys. Rev. A **101**, 013413 (2020).

[75] S. F. Vázquez-Carson, Q. Sun, J. Dai, D. Mitra, and T. Zelevinsky, Direct laser cooling of calcium monohydride molecules, arXiv preprint arXiv:2203.04841 (2022).